

Chromosomal replication initiates and terminates at random sequences but at regular intervals in the ribosomal DNA of *Xenopus* early embryos

Olivier Hyrien and Marcel Méchali

Unité d'Embryologie Moléculaire, Institut Jacques Monod,
2 Place Jussieu, 75 251 Paris Cedex 05, France

Communicated by M. Yaniv

We have analysed the replication of the chromosomal ribosomal DNA (rDNA) cluster in *Xenopus* embryos before the midblastula transition. Two-dimensional gel analysis showed that replication forks are associated with the nuclear matrix, as in differentiated cells, and gave no evidence for single-stranded replication intermediates (RIs). Bubbles, simple forks and double Ys were found in each restriction fragment analysed, showing that replication initiates and terminates without detectable sequence specificity. Quantification of the results and mathematical analysis showed that the average rDNA replicon replicates in 7.5 min and is 9–12 kbp in length. This time is close to the total S phase duration, and this replicon size is close to the maximum length of DNA which can be replicated from a single origin within this short S phase. We therefore infer that (i) most rDNA origins must be synchronously activated soon in S phase and (ii) origins must be evenly spaced, in order that no stretch of chromosomal DNA is left unreplicated at the end of S phase. Since origins are not specific sequences, it is suggested that this spatially and temporally concerted pattern of initiation matches some periodic chromatin folding, which itself need not rely on DNA sequence. **Key words:** early development/nuclear matrix/replication origins/ribosomal genes/two-dimensional agarose gel electrophoresis

Introduction

Eukaryotic DNA replication initiates at discrete sites irregularly spaced along chromosomal DNA molecules, and terminates by convergence of replication forks emanating from adjacent origins (Huberman and Riggs, 1968). In the yeast *Saccharomyces cerevisiae*, initiation sites correspond to specific nucleotide sequences. Some, but not all, *S. cerevisiae* DNA fragments can confer to circular plasmids autonomous replication into yeast cells (Stinchcomb *et al.*, 1979). Two-dimensional (2D) gel electrophoretic analysis confirmed that initiation occurs on plasmids at these yeast autonomously replicating sequence (ARS) elements (Brewer and Fangman, 1987; Huberman *et al.*, 1987). Many, though not all, ARS elements are also active as origins in the chromosome [reviewed in Fangman and Brewer (1991, 1992)]. A complex of six polypeptides that binds ARS elements *in vitro* and *in vivo* has recently been isolated (Bell and Stillman, 1992; Diffley and Cocker, 1992), sharpening the notion that initiation of DNA replication in yeast cells is performed by a sequence-specific origin recognition complex.

2D gel analysis also demonstrated that termination occurs at a specific site in the *S. cerevisiae* ribosomal DNA (rDNA) cluster, due to the presence of a polar replication fork barrier at the 3' end of the 35S rRNA transcription unit (Brewer and Fangman, 1988; Linskens and Huberman, 1988). By contrast, converging replication forks emanating from two adjacent origins on *S. cerevisiae* chromosome III terminate non-specifically, wherever they happen to meet, in a broad zone of at least 4.3 kbp (Zhu *et al.*, 1992a).

In multicellular eukaryotes, there is no decisive evidence that a restricted set of specific sequences comparable to yeast ARS elements act either as *cis*-determinants of origin function or as sites for the initiation of DNA synthesis. Even less is known about their termination sites. In the frog *Xenopus laevis*, any plasmid molecule injected into unfertilized eggs replicates under cell cycle control with an efficiency which depends only upon the size of the plasmid and not on the presence of any particular DNA sequence (Harland and Laskey, 1980; Méchali and Kearsley, 1984). 2D gel analyses confirmed that initiation and termination occur on plasmids without detectable sequence specificity in eggs or egg extracts; they also disclosed that only a single randomly situated initiation event takes place on each plasmid molecule despite the abundance of potential origins (Hyrien and Méchali, 1992; Mahubani *et al.*, 1992). However, the relevance of these findings for other cell types was not obvious, because amphibian eggs are specialized cells primed for the very rapid cell cycles that follow fertilization. Interestingly, any human DNA fragment of sufficient length is able to confer autonomous replication in human cells when inserted into a non-replicating, EBV-derived vector which is deleted for the dyad region of the EBV origin (Heinzl *et al.*, 1991). Replication initiates in these recombinants at multiple locations both on the vector and insert sequences (Krysan and Calos, 1991). These results and subsequent studies (Caddle and Calos, 1992; Tran *et al.*, 1993) convincingly showed that a relaxed sequence specificity for initiation on plasmids is not a unique feature of amphibian eggs.

Plasmid replication may not necessarily mimic chromosomal replication. Random initiation was reported for the tandem repeats of histone genes in *Drosophila* embryos (Shinomiya and Ina, 1991). However, various studies of rRNA genes in numerous species (references in Hernandez *et al.*, 1993), including embryos of *Drosophila* (McKnight *et al.*, 1978), sea urchin (Botchan and Dayton, 1982) and *Xenopus* (Bozzoni *et al.*, 1981), suggested the presence of a specific origin of replication in the intergenic spacer of the rDNA repeat units. Furthermore, some recently developed replicon mapping techniques suggested that initiation only occurs at a short DNA region within the DHFR domain in Chinese hamster ovary (CHO) cells (Burhans *et al.*, 1990; Vassilev *et al.*, 1990). In contrast, a systematic 2D gel electrophoretic analysis rather suggested that initiation can occur at any of a large number of sites

scattered throughout a 55 kbp zone downstream of the DHFR gene (Vaughn *et al.*, 1990a; Dijkwell and Hamlin, 1992). This controversy led to speculation about the nature of initiation intermediates at this locus [reviewed and discussed by Linskens and Huberman (1990), Hamlin (1992) and DePamphilis (1993)]. Dispersive initiation within a broad but circumscribed zone also occurs in the process of chorion gene amplification in *Drosophila* follicle cells (Delidakis and Kafatos, 1989; Heck and Spradling, 1990) and at a *Schizosaccharomyces pombe* origin (Zhu *et al.*, 1992b).

Conventional replication intermediates (RIs) consist of forks in which the synthesis of both nascent strands is tightly coupled to the unwinding of parental duplex DNA. However, an absence of replication forks and a concomitant abundance of long single-stranded DNA stretches were observed by electron microscopy in the chromosomal DNA of *Xenopus* embryos (Gaudette and Benbow, 1986). These authors proposed that parental strands may undergo extensive separation prior to any daughter strand synthesis during chromosomal replication in *Xenopus* [reviewed in Benbow *et al.* (1992)].

2D gel analyses of plasmids replicating in *Xenopus* eggs or egg extracts (Hyrien and Méchali, 1992; Mahbubani *et al.*, 1992) did not support mechanisms involving abundant single-stranded intermediates; nor did they provide evidence for specific initiation or termination in the *Xenopus* rDNA repeat. It was therefore necessary to clarify whether the mechanism and sequence specificity of initiation on *Xenopus* chromosomal DNA sequences differed from that of plasmids. We report here a 2D gel analysis of the replication of the chromosomal rDNA cluster in *Xenopus* embryos before the midblastula transition (MBT; Signoret and Lefresne, 1971; Newport and Kirschner, 1982), when rapid replication occurs in the absence of detectable transcription. We have also performed a detailed quantitation of plasmid and chromosomal replication intermediates and developed a theoretical model to analyse and compare these data.

Results

Strategy for replicon mapping of the *X.laevis* rDNA cluster by 2D gel electrophoresis

In the 2D gel electrophoretic technique of Brewer and Fangman (1987, 1988; Figure 1), replication fork-containing restriction fragments are separated from linear restriction fragments by two consecutive electrophoreses in agarose gels and examined after Southern blotting and hybridization to an appropriate probe. The first electrophoresis is run under conditions in which restriction fragments are separated according to mass only, while the second electrophoresis uses conditions which maximize the contribution of shape to migration rates, causing replication intermediates to migrate more slowly than linear fragments of the same mass, according to the number and position of replication forks they contain. Each class of replication intermediates thus traces a particular pattern (Figure 1), allowing the determination of whether the fragment is replicated by either a single fork (Y-shaped RIs), or two diverging forks initiated within the fragment (bubbles, or O-shaped RIs), or two converging forks terminating within the fragment (double Ys, or H-shaped RIs).

The *X.laevis* genes coding for the 40S rRNA precursor (reviewed by Reeder, 1990) are arranged as a single tandem

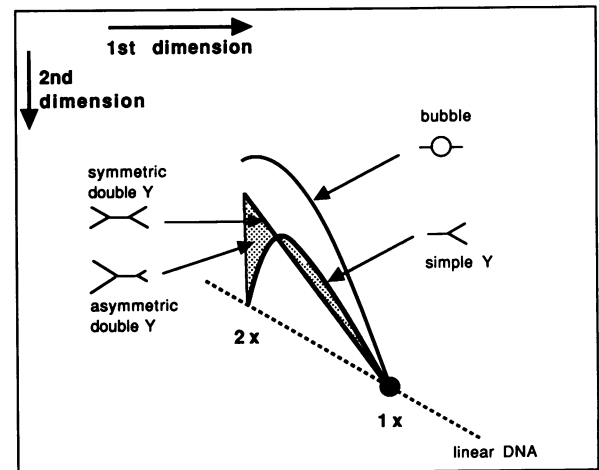


Fig. 1. 2D gel patterns generated by the three basic forms of replication intermediates. The principle of the technique is described in the text. For a detailed explanation of arc shapes, see Fangman and Brewer (1991) and Hyrien and Méchali (1992).

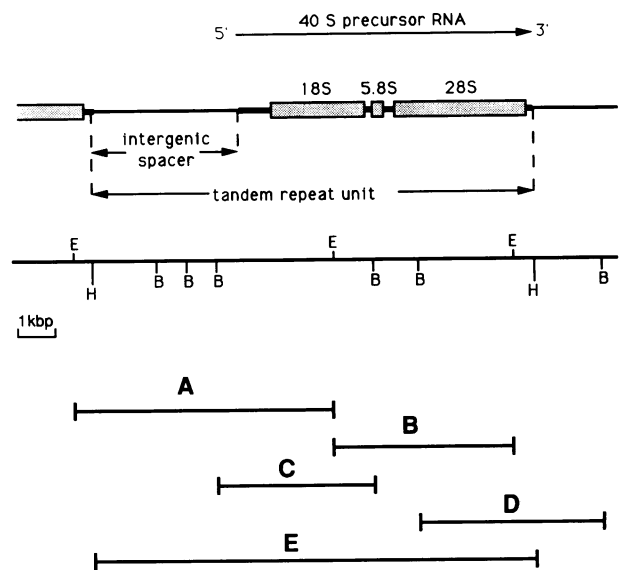


Fig. 2. Maps of *X.laevis* rDNA. Structure of the repeat unit (top), restriction map (middle), and restriction fragments analysed (bottom). Symbols on the restriction map are E: *Eco*RI; B: *Bam*HI; H: *Hind*III.

of a 11–15 kbp unit repeated 400 times. A map of the rDNA tandem repeat unit and the overlapping restriction fragments analysed here is presented in Figure 2. Each rDNA tandem repeat unit comprises a 7.7 kb rRNA transcription unit which is separated from the next by an intergenic spacer of variable length (3–7 kbp). This length polymorphism, which is due to the presence of various numbers of repetitive elements, is reflected in a size variation of fragments A and E, and to a lesser extent fragment C.

In addition to chromosomal copies, the *Xenopus* oocyte contains amplified extrachromosomal rDNA, which is slowly degraded during cleavage but persists until the early gastrula stage. However, the remaining rDNA does not seem to be associated with nuclei (Busby and Reeder, 1982) and is presumably lost during nuclear matrix isolation (see below). Furthermore, it is not replicated in the early embryo (Busby and Reeder, 1982) and therefore does not contribute to the signals detected on 2D gels.

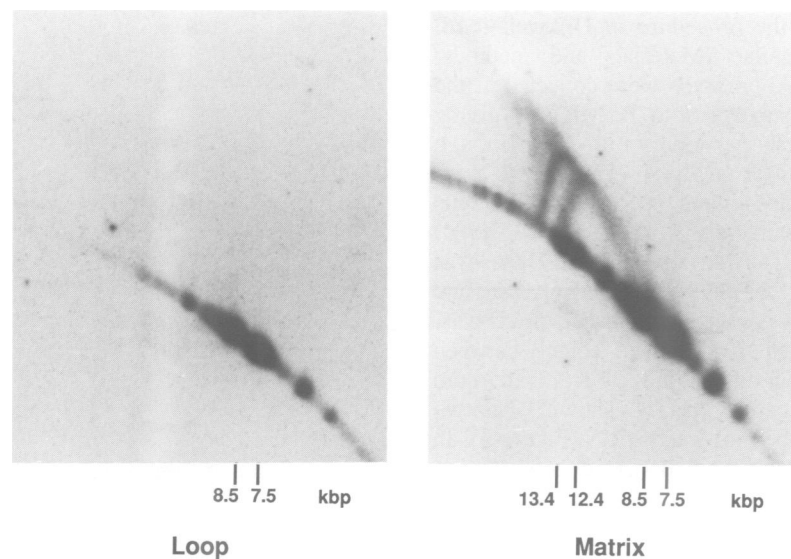


Fig. 3. Replication forks are associated with the nuclear matrix in early *Xenopus* embryos. Nuclear haloes were digested with *EcoRI*, and matrix-associated DNA was separated from detached (loop) DNA by centrifugation. The two fractions were subjected to 2D gel electrophoresis, and the gels blotted and probed for restriction fragment A (see Figure 2) as indicated in Materials and methods. The two film exposures are identical. Longer exposures of the matrix blot are provided in Figure 4A and 4A'.

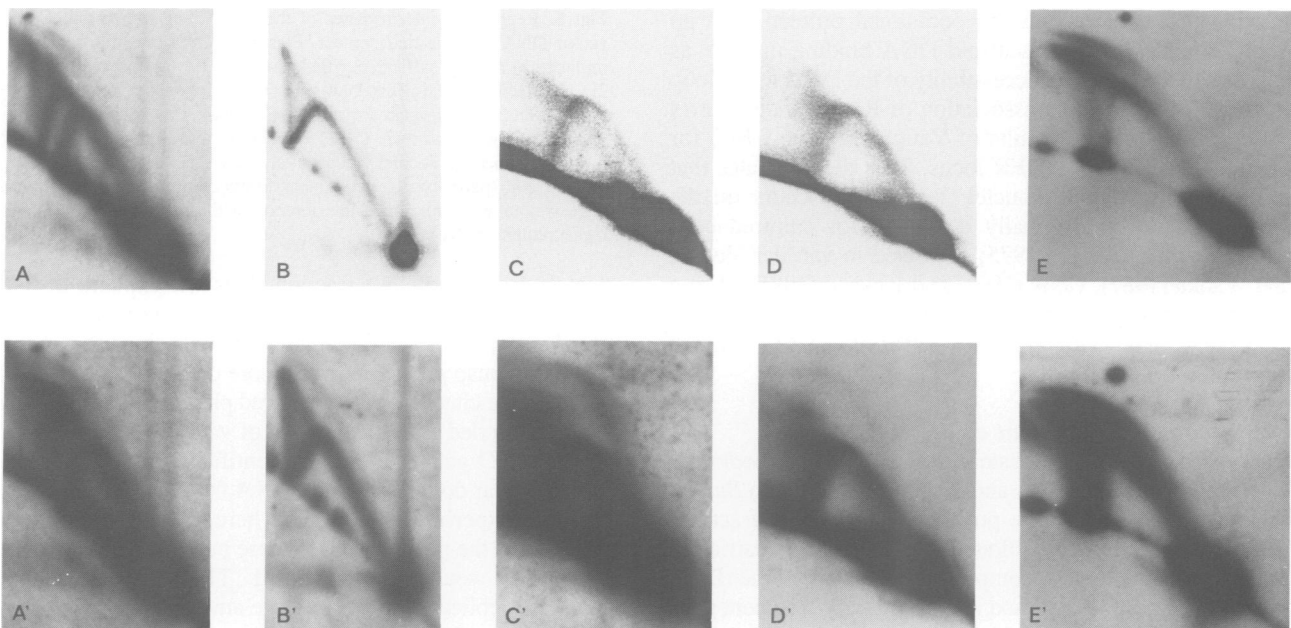


Fig. 4. Detection of *Xenopus* rDNA replication intermediates isolated on the nuclear matrix. Blots of matrix-associated DNA were prepared after digestion of nuclear haloes with *EcoRI* (A, B) or *BamHI* (C, D) or *HindIII* (E). The capital letter (A, B, C, D, E) indicates the fragment probed according to the map in Figure 2. Panels A', B', C', D' and E' are longer exposures of panels A, B, C, D and E. A lower exposure of panel A blot is also provided in Figure 3.

Stabilization of replication intermediates by isolation on the nuclear matrix in early *Xenopus blastulae*

In our preliminary attempts to analyse the replication intermediates of the *X. laevis* rDNA cluster, total DNA was purified from a few hundred embryos at the 1000–2000 cell stage by a standard phenol–chloroform extraction method. Such samples only allowed the visualization of faint, often smeared Y arcs. We next tried increasing the number of embryos used and enriching for rDNA sequences by isopycnic centrifugation of purified DNA on CsCl gradients. However, fragment A consistently gave uninterpretable smears, and only the largest bubbles were detected in

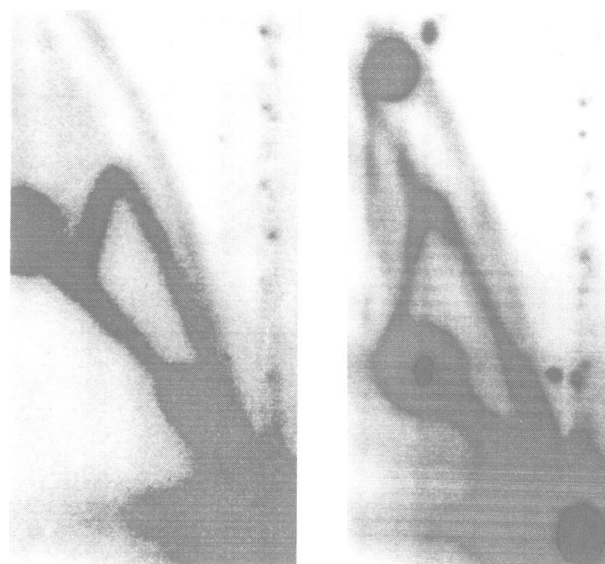
addition to Ys and double Ys in the other fragments (data not shown). Furthermore, the amount of bubbles was much too low to account for the high density of replication origins expected in these very rapidly dividing embryos. Similar difficulties reported during the study of the CHO DHFR locus were largely solved by isolation of replication intermediates on the nuclear matrix (Dijkwel *et al.*, 1991), a procedure which eliminates shearing and branch migration of RIs by keeping the chromosomal DNA in the form of affixed supercoiled loops. However, it was uncertain whether replication occurred on a similarly defined matrix in *Xenopus* early embryos.

We therefore adapted the procedure of Dijkwel *et al.* (1991) to *Xenopus* blastulae (Materials and methods; Figure 3). A total of 2200 embryos were collected at the 1000–2000 cell stage, a stage prior to the MBT but giving a sufficient number of cells per embryo to obtain enough replication intermediates for analysis. The nuclei were purified, the nuclear haloes were prepared by isotonic lithium–diiodosalicylate extraction (Mirkovitch *et al.*, 1984) and digested with *Eco*RI. Matrix-associated DNA was separated from detached (loop) DNA by centrifugation, and the two purified fractions were separately loaded on 2D gels. The linear DNA partitioned approximately equally between the loop and matrix fraction, as judged from ethidium bromide staining of the agarose gels (not shown). The two gels were blotted and probed for fragment A (Figure 3). In this batch of embryos, fragment A occurred in two major size variants (7.5 and 8.5 kbp) that again partitioned in equal amounts between the two fractions. However, all classes of replication intermediates, as well as linear partial digests (12.4 and 13.4 kbp, and above), partitioned exclusively to the nuclear matrix (Figure 3; see also Figure 4A and 4A'). Reprobing these two blots with fragment B gave identical results (matrix blot shown in Figure 4B and 4B'). The exclusive association of linear partial digests with the matrix fraction probably reflects the occasional protection of an *Eco*RI site by a nuclear scaffold DNA binding protein, as opposed to the complete accessibility of the DNA in the loop fraction. The exclusive association of RIs with the matrix is consistent with the results of Vaughn *et al.* (1990b) for the Chinese hamster DHFR locus. This demonstrates that in embryonic *Xenopus* nuclei, replication occurs on the nuclear matrix as originally described for cultured cells [Berezney and Coffey, 1975; reviewed in van der Velden and Wanka (1987), Cook (1991) and Jackson (1991)]. From a practical standpoint, this has allowed us to study *Xenopus* embryonic RIs with minimal shearing and/or branch migration.

Every restriction fragment of the rDNA cluster displays all types of classical replication intermediates

Nuclear haloes prepared as above were digested with *Bam*HI or *Eco*RI or *Hind*III. The purified matrix DNA fractions were loaded on 2D gels, blotted and probed for restriction fragments A–E, to get a comprehensive picture of the rDNA locus RIs (Figure 4A–E and A'–E'). Every fragment gave a complete and continuous Y arc, a complete and continuous bubble arc, and a triangular smear of symmetric and asymmetric termination intermediates. The bubble arcs from the two main size variants in Figure 4A (7.5 and 8.5 kb) are fused together at their top, but can be separately tracked down just below. Despite the fact that fragments A–D overlap with each other and completely cover the rDNA repeat unit, the amount of bubbles seemed low in every fragment when compared with the amount of double Ys. This was puzzling since the number of initiation and termination events per repeat unit must be the same. Furthermore, short bubbles were strongly underrepresented in the bubble arc of fragment E. These two oddities are addressed in detail in a later section.

The small amounts of additional material on the left of the triangular smear of fragment A and fragment E arise from the minor spot(s) of linear partial digests; they represent the partially digested standard RIs that are expected in the



B insert

ColE1 vector

Fig. 5. Replication intermediates of the rDNA fragment B and ColE1 vector DNA in a plasmid context. Plasmid pXlr11 was allowed to replicate in an egg extract, purified, cut with *Eco*RI and subjected to 2D gel electrophoresis. The blot was probed for insert fragment B, stripped and probed again for the ColE1 vector fragment. The round spot under the apex of the ColE1 bubble arc and the additional spot on the arc of linear molecules, respectively, correspond to the nicked circular and (partially digested) linear forms of the plasmid monomer. Care was taken to minimize interference of these spots with measurement of RI arcs.

matrix-associated DNA fraction. This also explains the light background smear to the left of the linear monomer spot on the *Bam*HI digest (fragments C and D), since the *Bam*HI restriction map predicts a much more complex set of partials.

We have checked with denatured phage lambda DNA that single-stranded DNA fragments of various lengths migrate on these 2D gels as a clearly identifiable arc distinct from that of linear double-stranded DNA fragments (not shown). For the experiments presented here, no signal was ever detected at the position where these putative single-stranded molecules would have migrated. Thus, the detection of standard replication forks in large amounts and the absence of any new 2D gel pattern fail to support the electron microscopy results of Gaudette and Benbow (1986). Furthermore, the presence of each complete class of standard RIs in each fragment analysed demonstrates that replication initiates and terminates at multiple, apparently random positions on the chromosomal rDNA sequences of *Xenopus* embryos at the 1000–2000 cell stage. No pattern of specific initiation or replication fork barrier was observed, in contrast to the situation found in the rDNA of yeast (Brewer and Fangman, 1988; Linskens and Huberman, 1988) or pea (Hernandez *et al.*, 1993).

Quantitative analysis of replication intermediates: application to an rDNA plasmid

The recent advent of storage phosphor technology now makes possible precise signal quantifications from areas of any shape on an autoradiogram. The relative amounts of the various classes of RIs of a given fragment reflect the

Table I. Quantitation of replication intermediates of the B ribosomal insert and ColE1 vector fragments in pXlr11 and calculations of replicon size

Restriction fragment	Fragment size	Percent of total RIs			H/O ratio	Calculated replicon size (kbp)	
		O	H	Y		from Y/O	from Y/H
B insert	4.9	9.6	13.9	76.5	1.45	13.6	12.4
ColE1	6.4	14.7	17.1	68.2	1.16	13.0	13.5

Bubbles were measured for $0.3 < R < 1.0$ and double Ys for $0.5 < R < 1.0$. The values were then corrected according to equations (18) and (19) to derive the total amounts of each class of replication intermediate. Replicon sizes were calculated according to equations (16) and (17).

Table II. Quantitation of chromosomal replication intermediates and calculations of the chromosomal rDNA replicon size

Restriction fragment	Fragment size (kbp)	Percent of total RIs			H/O ratio	Calculated replicon size	
		O	H	Y		from Y/O	from Y/H
A	7.5–8.5	9.1	33.2	57.7	3.66	19.3	11.9
B	4.9	5.3	32.6	62.1	6.10	17.6	7.5
C	4.1–4.3	10.1	36.9	52.9	3.64	9.1	5.9
D	4.5	10.0	30.9	59.1	3.10	10.4	6.9
E	12.7–14.2	31.7	63.6	4.7	2.01	13.9*	13.8*

Measurements and data processing were as for Table I. The asterisk (*) indicates that replicon size calculations for fragment E may be not meaningful since equations (16) and (17) can be used to calculate replicon size only if $N > n$.

frequencies of initiation and termination within that fragment. We present in Materials and methods a mathematical analysis which allows the calculation of replicon size from the various RI ratios of its restriction fragments.

In order to assess the relevance of this model to experimental cases, we applied it to the study of a plasmid replicating in an egg extract. Plasmid pXlr11 consists of the ribosomal 4.9 kbp *EcoRI* fragment B inserted at the *EcoRI* site of the 6.4 kbp ColE1 vector. A blot of 2D gel-resolved *EcoRI*-cut RIs of plasmid pXlr11 that had replicated in an egg extract was probed with fragment B, eluted and probed again with ColE1 (Figure 5). We first scanned small consecutive portions of the bubble arcs and plotted their intensities against replication extent (data not shown). The curves obtained closely fitted the theoretical curve defined by equation (5), thus justifying the use of equation (18) to calculate the intensity of the complete bubble arcs (see Materials and methods). Table I shows the relative amounts of each complete RI class derived from these measurements using equations (18) and (19), and the replicon size calculated from these relative amounts using equations (16) and (17). The H/O ratio is 1.45 (fragment B) or 1.16 (ColE1 vector). Both values are very close to the theoretical value (1.25) given by equation (13). This argues against any significant difference in the recovery of these two RI classes. The replicon sizes calculated from the Y/O ratio (13.6 or 13.0 kbp) or the Y/H ratio (12.4 or 13.5 kbp) are in every case good approximations of the exact plasmid size (11.3 kbp). This further reinforces the notion that the plasmid is a single replicon, in other words that replication initiates only once per plasmid molecule despite its richness in potential origins (Hyrien and Méchali, 1992; Mahubani *et al.*, 1992). The slight overestimation of the plasmid size could be explained by the known presence of contaminating dimer and higher multimer plasmid molecules which presumably also initiate replication only once per plasmid (Martin-Parras *et al.*, 1992). Our model can therefore confidently be used to

determine the size of a randomly initiating and terminating replicon.

Quantitative analysis of replication intermediates: application to the chromosomal rDNA sequences

We now turn to the quantitative RI analysis of chromosomal rDNA, beginning with fragments A–D. First, we scanned small consecutive portions of the bubble arcs and plotted their intensity against replication extent (data not shown). The curves obtained for fragments B, C and D compared reasonably well with the theoretical curve defined by equation (5), and only a small excess of the largest bubbles was apparent for fragment A. Second, we calculated as for plasmid RIs the amount of each class of RIs (Table II); the H/O ratio was 2.5- to 5-fold higher than expected for fragments A–D. This discrepancy with the theoretical model was not observed with rDNA plasmids (Figure 5 and Table I; see also Hyrien and Méchali, 1992).

These abnormal H/O ratios could be artefactual due to a less than optimal preservation of bubbles, especially small ones, when isolated from chromosomal DNA but not plasmid DNA. Alternatively, the excess of double Ys to bubbles could reflect that at least one of the hypotheses of the model is not valid for chromosomal DNA. One assumption of the model is that the fragment under study is smaller than the complete replicon. This condition is fulfilled for each of fragments A–D, as Ys would be very rare in the opposite case. The second possibility is that some sites may be disfavoured for initiation; however, this would not explain why every fragment shows an elevated H/O ratio. The remaining possibility is that chromosomal replication may not proceed with a constant speed from initiation to termination, contrary to plasmid DNA. RIs displayed by fragments smaller than the replicon are necessarily biased towards the earliest bubbles and latest double Ys. Therefore, the deviation of the H/O ratio observed with fragments A–D would be explained if replication proceeds faster around

initiation than around termination. In this case, the H/O ratio should be highest for the smallest fragments, and reach a minimal value for fragments the size of the replicon. For theoretical reasons not detailed here [but which can be derived by appropriate modifications to equations (5) and (6)], this minimal value would now be >1.25 .

Several strong predictions can be made for RIs of fragments equal to or slightly larger than the replicon. First, simple Ys should virtually disappear: RIs should only consist of bubbles and double Ys, plus trace amounts of triple- and quadruple-forked molecules. Second, the bias towards the earliest bubbles and latest double Ys should have disappeared, resulting in an H/O ratio equal to the minimum value discussed above; there should now be a deficit in both early bubbles and early double Ys, and an excess of late RIs of both classes.

The RIs of fragment E meet all these predictions (Figure 4E and Table II). The very small amount of Ys ever observed is consistent with very few rDNA replicons being larger than fragment E. A strong deficit in both early bubbles and early double Ys ($R < 0.5$) is apparent by visual inspection (Figure 4E), and was confirmed when small consecutive portions of these arcs were scanned and their intensity plotted against replication extent (data not shown). Again, this did not appear when the same fragment was replicated in a plasmid context (Hyrien and Méchali, 1992). Finally, the observed H/O ratio for fragment E is only 1.6-fold higher than expected, and is the smallest of all rDNA fragments.

Owing to the peculiarities of chromosomal RIs explained above, caution must be exercised in estimating replicon size (Table II). If an artefactual loss of the shortest bubbles has occurred, the true replicon size is best estimated from the Y/H ratios of fragments A–D (8.7 kbp on size-weighted average). If the replication speed varies as discussed above, the true replicon size must lie somewhere between this value and that estimated from the Y/O ratios (15.0 kbp on size-weighted average). The very small amount of Ys observed for fragment E shows that most rDNA replicons are not larger than 12–14 kbp, which is consistent with both these estimates.

Our data suggest a somewhat higher frequency of both initiation and termination in *Bam*HI fragments C and D than in *Eco*RI fragments A and B. The higher H/O ratio found for fragment B also suggests that termination is slightly more frequent in the transcription unit sequences than in the rest of the rDNA repeat. However, we cannot exclude a slight variation from blot to blot in the yield or detection of various classes of RIs.

The fork rate in *Xenopus* somatic cells and egg extracts has previously been estimated to be 600 bp/min (Callan, 1972; Mahbubani *et al.*, 1992), and the S phase at the developmental stage investigated here has been considered to last no more than 10 min (Graham and Morgan, 1966), although we estimated that it was somewhat longer (12–16 min; see Materials and methods). These values imply that replicons must be smaller than 12–20 kbp. The comparison with our estimates of the average rDNA replicon size suggests that their size distribution must be much more homogeneous than if initiation was an entirely stochastic process, otherwise replication could not be completed before the end of the S phase.

Quantitation of the RI-to-linears ratio: estimating the rDNA replication timing

The time fraction of the cell cycle taken to replicate a fragment is reflected in the relative abundance of its branched and linear forms. The signal from total RIs and from linears was measured on the *Hind*III blot (Figure 4E). After correction for the amount of linears remaining in the loop fraction, the RI percentage found is 30%. The cell cycle in our experimental conditions is ~ 25 min long. Thus, the replication time span of rDNA sequences is at least 0.3×25 min = 7.5 min. An independent estimate of the rDNA replicon size is given by the product of this time and the replication speed: 7.5 min \times 0.6 kbp/min/fork \times 2 forks/replicon = 9 kbp. This value is in very good agreement with the previous estimate from the Y/H ratio, which also relied upon the assumption of a constant replication speed. First, this suggests that we had a nearly complete RI recovery in this experiment. Second, this timing implies, assuming a 12–16 min S phase, that most initiation events occur within the first 4–8 min of S phase, and that termination occurs within the last 4–8 min.

Discussion

The nature of replication intermediates in the chromosomal rDNA cluster during Xenopus early development

Our results show that replication of the chromosomal rDNA cluster in *Xenopus* cleavage embryos proceeds by classical replication forks present in normal amounts, and provide no evidence for atypical RI containing long stretches of single-stranded DNA. These results conflict with the electron microscopy observation that classical replication forks are absent while lengthy single-stranded segments are abundant in total DNA from *Xenopus* embryos (Gaudette and Benbow, 1986; reviewed in Benbow *et al.*, 1992). We do not believe that rDNA is a special case unrepresentative of the replication mode of the rest of the genome, since the ethidium bromide-stained gels also failed to show any material at the position expected of single-stranded DNA, and did show a light staining at the position expected of classical replication intermediates of the whole genome, i.e. in a wide area above the diagonal track of linear molecules. Pulse–chase experiments with replicating sperm nuclei in an egg extract confirmed that all detectable RIs of the whole genome migrate at this position on 2D gels (data not shown).

2D gel analysis of pea rDNA replicons has recently led to a similar controversy. Van't Hof and Lamm (1991) detected atypical intermediates of single-stranded character and suggested that rDNA replicates by displacement loops. However, classical replication forks were observed in pea rDNA by Hernandez *et al.* (1993), who suggested that the single-stranded molecules rather resulted from degradation of RIs during isolation of DNA or from contaminating extrachromosomal rDNA.

We noted a deficit in bubbles, especially smaller ones, even though the nuclear matrix isolation procedure of Dijkwel *et al.* (1991) was used. Does this reflect the greater instability of small bubbles or some misunderstood feature of chromosomal replication? While we have no decisive evidence to exclude the first hypothesis, it is not supported by the fact that plasmid RIs displayed the expected amount

of bubbles of all sizes. This result suggests that a quantitative retention even of the shortest detectable bubbles, both before and after restriction enzyme digestion, is not intrinsically difficult, especially since RI isolation was far less gentle for plasmid than for chromosomal DNA. Moreover, recent evidence that RI are stable for hours at 37°C challenged the view that uncatalysed branch migration is a fast and efficient process (Müller *et al.*, 1992). A specific loss of short bubbles from chromosomal RIs on the nuclear matrix cannot be disproven, but seems unlikely since replication forks were quantitatively retained on the nuclear matrix, and thus presumably protected against breakage and/or branch migration.

The detailed quantitative RI analysis of all rDNA chromosomal restriction fragments is entirely consistent with an alternative hypothesis: chromosomal replication might proceed faster around initiation than around termination. This may be achieved by the simultaneous formation of multiple, small replication bubbles in a circumscribed initiation zone. Indeed, clusters of microbubbles have been observed by electron microscopy in a variety of sources, including whole DNA and rDNA of *X. laevis* embryos, and were postulated to represent an early stage of chromosomal DNA replication (Baldari *et al.*, 1978; Bozzoni *et al.*, 1981; Micheli *et al.*, 1982). How they migrate on 2D gels is not known. Since we found no evidence for a novel RI arc, they may be difficult to resolve from other early RIs. Alternatively, variations in the replication fork speed during chromosomal replication could be a mechanistic consequence of topological problems that do not arise during replication of small supercoiled plasmids. It is important to stress again that plasmid RIs displayed the expected amount of bubbles of all sizes. We feel that the mathematical tools provided here may help 2D gel interpretation in other experimental systems.

The absence of sequence specificity for initiation and the structural control of origin spacing

Our results establish that replication can initiate and terminate at any DNA sequence throughout the rDNA cluster, extending to chromosomal DNA the conclusions previously drawn for plasmid replication in *Xenopus* (Hyrien and Méchali, 1992; Mahbubani *et al.*, 1992). Detailed quantitations (Table II) nevertheless suggested a slightly higher frequency of both initiation and termination around both ends of the rRNA transcription unit, and a balance slightly shifted towards termination rather than initiation within the transcription unit sequences.

The lack of sequence specificity for initiation raises a problem. If initiation was an entirely stochastic process, it would occur at intervals that form a Poisson distribution around the mean replicon size and there would be a significant number of cases where the distance between adjacent origins would be too long to allow complete replication within the very short S phases of the early blastula (Laskey, 1985). Two features of chromosomal rDNA replication strongly suggest that adjacent initiation events do not occur independently of each other, but in a highly concerted fashion both spatially and temporally. First, the replication time span we found (at least 7.5 min) is a large fraction of S phase length, suggesting activation of all rDNA origins in a restricted temporal window in the first half of

S phase. Second, we found that the rDNA replicon size distribution is closely centred around 9–12 kbp, despite the abundance of sites capable of supporting initiation. We therefore suggest that initiation is random with respect to DNA sequence, but not random with respect to some periodic architecture of the chromatin fibre, such as its organization in consecutive loops of rather uniform size.

Interestingly, the replicon size we found is close to the probable size of chromatin loops in *Xenopus* blastulae (Buongiorno-Nardelli *et al.*, 1982; O. Hyrien, unpublished results). Our observation that replication forks partitioned exclusively to the nuclear matrix in early embryos is consistent with models in which replicating loops are reeled through matrix-bound replication complexes [Pardoll *et al.*, 1980; Buongiorno-Nardelli *et al.*, 1982; reviewed in van der Velden and Wanka (1987), Cook (1991) and Jackson (1991)]. According to these models, permanent nuclear matrix attachment sites coincide with the loop replication initiation sites. They may therefore occur in *Xenopus* cleavage nuclei at random positions instead of at classical MAR/SAR sequences. We are currently examining this interesting possibility.

Chromosomal replication occurs at 100–300 discrete foci, each of which contains numerous replication forks clustered together (Nakamura *et al.*, 1986; Hutchinson and Kill, 1989; Mills *et al.*, 1989; Nakayasu and Berezney, 1989). Interestingly, the assembly of replication foci in *Xenopus* egg extracts does not rely on any specific DNA sequence (Cox and Laskey, 1991) and takes place before initiation proceeds (Kill *et al.*, 1991; Adachi and Laemmli, 1992). If periodically folded, a chromatin fibre could establish regular points of contact with the replication foci at the onset of S phase. Concerted initiation at these contact points would ensure non-random origin spacing without sequence specificity. Supporting this view is the observation that initiation in *Drosophila* cleavage embryos occurs at intervals that are integral multiples of 3.4 kbp (Blumenthal *et al.*, 1973), despite an apparent absence of sequence specificity for initiation (Shinomiya and Ina, 1991). Thus, regulation of chromatin folding may control origin spacing.

The absence of a replication fork barrier in rDNA during early development

In the yeast rDNA cluster, forks moving opposite to the direction of 35S RNA transcription are prevented from entering the active transcription units by a polar replication fork barrier (RFB) located at their 3' end. Recent evidence (Brewer *et al.*, 1992; Kobayashi *et al.*, 1992) demonstrated that this barrier functions independently of the act of transcription and may be due to the binding of an unidentified protein to a specific DNA sequence at the 3' end of the unit. Interestingly, a similar RFB has been found in pea rDNA (Hernandez *et al.*, 1993). However, we found no evidence for an RFB in the rDNA locus of *Xenopus* early blastulae. Convergent forks initiated from adjacent origins rather appear to terminate wherever they happen to meet. Transcription of the *Xenopus* rDNA genes is not yet active at the developmental stage examined here. It is therefore possible that the expression or activation of the putative RFB binding protein occurs later, at the time rRNA transcription is turned on, perhaps in conjunction with origin specification in the rDNA cluster.

Modulations in chromatin structure and replication origin specificity in higher eukaryotes

Our results demonstrate that chromosomal DNA replication can occur without specific initiation or termination sequences. So why does replication only start at a set of fixed locations in other instances? The answers probably reside in the fact that DNA duplication is not the sole event taking place in S phase; chromatin assembly coupled to DNA replication and associated opportunities to stably propagate or reprogramme gene activity also take place throughout S phase (Wolffe, 1992). In *S. cerevisiae* (Fangman and Brewer, 1991) and *Physarum* (Bénard and Pierron, 1992), the task of duplicating a rather short genome with a limited capacity for alternative differentiated states may be simplified by the use of rigidly defined sequences. The situation is different in multicellular eukaryotes, whose genomes are larger and experience a much wider variety of structural and functional diversifications associated with development and differentiation. This may render impracticable the use of rigidly fixed origins.

Replication in higher eukaryotes may rather exploit transcription-associated changes in chromatin structure to define initiation sites. For example, the boundaries of the CHO DHFR locus initiation zone coincide with the 3' ends of two convergently oriented transcribed genes (Dijkwel and Hamlin, 1992). Moreover, numerous examples of functional overlap between replication and transcription (Heintz, 1992; Heintz *et al.*, 1992) suggest that transcription factors might serve to target appropriate regions of the genome to different subclasses of replication centres with different chromatin assembly properties. The formation and disappearance of these different classes of replication centres may take place at different times within a single S phase, as suggested by the general correlation between transcriptional activity and replication timing in higher eukaryotes (Goldman, 1988; Fangman and Brewer, 1992).

In this hypothesis, changes in the position of initiation sites are likely to occur during the development of multicellular eukaryotes. Changes in origin density have been documented in *Drosophila* (Blumenthal *et al.*, 1973) and in *Triturus* (Callan, 1972), but origin specificity was not addressed in these studies. The transcriptional quiescence of early *Xenopus* embryos may simplify the task of chromatin replication to the point where it can occur by synchronous activation of closely spaced origins with no regard to specific sequences. At the midblastula transition (Signoret and Lefresne, 1971; Newport and Kirschner, 1982), the cell cycle slows down and transcription of many genes resumes, including the ribosomal genes (Shiokawa *et al.*, 1981). The midblastula transition might also be the time when specific origins are defined. Consistently, a circumscribed zone of initiation has been observed in the intergenic spacer of *X. laevis* rDNA at a later developmental stage (Bozzoni *et al.*, 1981). We are now trying to identify any changes in rDNA replication that may take place throughout *Xenopus* development.

Materials and methods

Buffers, plasmids and probes

Barth's consisted of: 15 mM Tris-Cl (pH 7.6), 88 mM NaCl, 2 mM KCl, 1 mM MgCl₂, 0.5 mM CaCl₂. Embryo Wash Buffer (EWB): 10 mM K-HEPES (pH 7.7), 100 mM KCl, 50 mM sucrose, 1 mM MgCl₂, 0.1 mM CaCl₂. TE: 10 mM Tris-Cl (pH 8.0), 1 mM EDTA. Nuclear Wash

Buffer (NWB): 5 mM Tris-HCl (pH 7.4), 50 mM KCl, 0.5 mM K-EDTA, 0.05 mM spermidine, 0.125 mM spermidine, 0.5% thiodiglycol, 0.25 mM phenylmethylsulphonyl fluoride, 0.1% digitonin (Fluka).

Cloned *X. laevis* rDNA was derived from plasmids pXlr11 and pXlr14 (Botchan *et al.*, 1977) and pXlr101A (Bakken *et al.*, 1982). Various subfragments were further subcloned into Bluescript M13+ by standard methods (Sambrook *et al.*, 1989). *EcoRI* blots were probed with labelled A or B fragments from pXlr11 or pXlr14, *HindIII* blots with labelled pXlr101A. To avoid cross-hybridization to non-cognate fragments through repetitive spacer sequences, *BamHI* blots were probed with the 2.45 kbp *XbaI*-*BamHI* subfragment on the right-side half of fragment C or the 2.3 kbp *BamHI*-*EcoRI* subfragment on the left-side half of fragment D.

Preparation of synchronously developing embryos and estimation of cell cycle and S phase length

Xenopus females were induced to ovulate and eggs were fertilized *in vitro* and dejellied as described previously (Gurdon and Wickens, 1983). Embryos were allowed to develop in 0.1 × Barth's at 23°C to the 1000–2000 cell stage. Abnormal or retarded embryos were discarded prior to batch collection. Owing to the metachronous pattern of cell divisions in each embryo (Satoh, 1977) and to small individual variations in cleavage rate, blastomeres are not synchronous in a batch of embryos even if collected at exactly the same time. From the time of the early cleavages we found an average cell cycle time of 25 min. We estimated S phase length by squashing 1000–2000 cell embryos stained with Hoechst under a microscope slide and counting interphase and mitotic nuclei. Consistent with other investigations (Montag *et al.*, 1988; Leibovici *et al.*, 1992), we found that S phase occupies one-half to two-thirds of the cell cycle, i.e. 12–16 min in our experimental conditions.

Stabilization and purification of total replication intermediates on the nuclear matrix

To prepare *Xenopus* embryonic nuclei suitable for nuclear matrix isolation, we devised the following procedure, which is an adaptation to early embryos of protocols used to prepare egg extracts (suggested to us by A.P. Wolffe). Batches of synchronously fertilized, dejellied embryos were collected as they reached the 1000–2000 cell stage and allowed to settle on ice. The embryos were rinsed four times with EWB by almost filling the tube and gently inverting it several times. Excess buffer was removed with a Pasteur pipette, and leupeptin and pepstatin were added to 10 µg/ml. The embryos were packed with a brief 700 g spin at 2°C, and excess buffer was removed again. The embryos were crushed by a 10 min 17 000 g spin at 2°C. This produced a dense insoluble plug of yolk platelets and pigments, a grey-brown liquid layer, a whitish liquid layer and a yellow plug of lipids. This has a very similar appearance to the extract obtained by the same procedure using unfertilized eggs. Both liquid layers were removed by side puncture of the tube with a 20 G needle. Phase contrast and Hoechst fluorescence microscopy examination showed the presence of the nuclei in both these liquid layers. The high viscosity of these undiluted cytoplasmic fractions probably accounts for the fact that nuclei did not sediment despite the high centrifugal force employed. The fractions containing the nuclei were mixed with an equal volume of glycerol, dropped in liquid nitrogen and stored at -80°C until further use. The number of recovered nuclei was estimated before or after freezing by counting an aliquot on a haematocytometer. Estimated yields varied from 50% to nearly 100%. This method therefore provides a simple and convenient way to prepare in very good yields embryonic nuclei free of yolk platelets and pigments.

Aliquots of frozen nuclei were thawed as needed and subjected to further purification essentially as described by Dijkwel *et al.* (1991). The thawed suspension was diluted in 10 vols of NWB and forced three times through a 21 G needle to free the nuclei from any cytoplasmic remnants. The nuclei were pelleted at 500 g for 5 min at 4°C, resuspended in 10 ml of NWB, layered over a 4 ml cushion of 12.5% glycerol in NWB, centrifuged for 10 min as above, and inspected and counted again by phase-contrast and fluorescence microscopy. Stabilization of the nuclei in CuSO₄ and isolation of RIs on the nuclear matrix were further performed exactly as described previously (method E in Dijkwel *et al.*, 1991), except that the final pellets were resuspended in 15 µl of TE and immediately used for 2D gel electrophoresis without further purification on BND-cellulose chromatography.

2D gel electrophoretic analysis

Neutral/neutral 2D gel electrophoresis was performed as described in Brewer and Fangman (1987), except that electrophoresis parameters were adapted to the size of the fragments analysed according to our previous observations with rDNA plasmids (Hyrien and Méchali, 1992). Electrophoresis in the first dimension was at room temperature, and in the second dimension in

a 4°C cold room in the presence of 0.3 µg/ml ethidium bromide with buffer recirculation, except for Figure 4E (room temperature). Conditions for Figure 3 and Figure 4A and B were first dimension in 0.3% agarose at 0.45 V/cm for 69 h and second dimension in 0.6% agarose at 2.25 V/cm for 20 h. Figure 4C and D: first in 0.3% agarose at 0.43 V/cm for 6 h, then at 0.33 V/cm for 63 h, and second in 1% agarose at 5 V/cm for 5 h. Figure 4E: first in 0.3% agarose at 0.35 V/cm for 95 h and second in 0.6% agarose at 1 V/cm for 44 h. Figure 5: first in 0.3% agarose at 1 V/cm for 19 h and second in 0.6% agarose at 2.25 V/cm for 17 h.

After migration, the gels were dephosphorylated in 0.25 M HCl, and DNA was transferred to Hybond N⁺ by alkali capillary blotting as recommended by the supplier (Amersham). Prehybridization (30 min) and hybridization (16–72 h) were performed at 42°C in 50% formamide, 5 × SSPE, 5 × Denhardt's, 1% SDS, 200 µg/ml denatured sonicated herring sperm DNA. Probes were labelled with [α -³²P]dATP and [α -³²P]dCTP to a specific activity of 1.2–2.6 × 10⁹ c.p.m./µg with a random primed DNA labelling kit (Amersham). After hybridization, the blots were washed in 2 × SSPE, 0.1% SDS twice for 10 min at 42°C and once for 30 min at 68°C, then in 0.1 × SSPE, 0.1% SDS twice for 30 min at 68°C. The washed blots were exposed to Amersham MP X-ray films at –70°C with two intensifying screens or to storage phosphor screens (Molecular Dynamics) for quantitative analysis.

Quantitation of all gels was by storage phosphor imaging using a Molecular Dynamics 400A PhosphorImager and the ImageQuant software. The areas of interest were integrated after background taken from an adjacent region of the gel (just above the bubble arc) was subtracted from the signal. The signal never exceeded the storage capacity of the screens.

Quantitative analysis of the different classes of replication intermediates: mathematical formalism

Let us consider an *N* bp circular replicon, in which initiation occurs at a single, randomly chosen location and replication proceeds with a constant fork speed to the termination site. In an asynchronously replicating population of such molecules, replication forks are randomly distributed along the replicon sequences, and all replicating plasmid configurations are equiprobable. We now calculate the relative amounts of various RIs found in an *n* bp fragment of the plasmid. Let us define *R* as the replication extent through the *n* bp fragment (0 < *R* < 1). We first calculate the number of all possible plasmid configurations where a single fork is in the *n* bp fragment, at a position defined by a given value of *R*. There are *N*–*n* possible positions for the fork outside the fragment; there is only one possible position, defined by *R*, for the fork inside the fragment; and there are two possibilities for deciding which fork is in the fragment; therefore:

$$N(Y_R) = 2(N-n) \tag{1}$$

We now calculate the number of plasmid configurations where the two forks are in a bubble configuration in the *n* bp fragment, at a given value of *R*. This is equal to the number of possible positions of the bubble within the fragment, which decreases with increasing bubble size, as expressed by:

$$N(O_R) = n(1-R) \tag{2}$$

We finally calculate the number of plasmid configurations with the two forks in a double-Y configuration in the *n* bp fragment, at a given value of *R*. This is equal to the number of possible positions of the two converging forks within the fragment, which increases with *R*, as expressed by:

$$N(H_R) = nR \tag{3}$$

The preceding equations described the relative number of molecules of each RI class at a given replication extent, i.e. of molecules that will migrate at a given position in a 2D gel. The signal intensity at any position within the gel is proportional to this number and, in the case of blot analysis, to the number of base pairs available for hybridization, which is equal to *n*(1 + *R*); hence:

$$I(Y_R) = N(Y_R) n(1 + R) = 2(N-n) n(1 + R) \tag{4}$$

$$I(O_R) = N(O_R) n(1 + R) = n^2 (1-R^2) \tag{5}$$

$$I(H_R) = N(H_R) n(1 + R) = n^2 (R^2 + R) \tag{6}$$

Since all replicating plasmid configurations are equiprobable, the signal for any portion (*R*₁ < *R* < *R*₂) of any RI arc is given by summing elementary signal intensities over the relevant *nR* interval (for simplification, replication is viewed as progressing continuously rather than by steps of one base pair):

$$S_{R1R2}(Y) = n \int_{R1 < R < R2} I(Y_R) dR \tag{7}$$

$$S_{R1R2}(O) = n \int_{R1 < R < R2} I(O_R) dR \tag{8}$$

$$S_{R1R2}(H) = n \int_{R1 < R < R2} I(H_R) dR \tag{9}$$

The total intensity of each arc (0 < *R* < 1) is given as a peculiar case of these equations by:

$$Y = n \int_{0 < R < 1} I(Y_R) dR = 3(N-n) n^2 \tag{10}$$

$$O = n \int_{0 < R < 1} I(O_R) dR = 2n^3/3 \tag{11}$$

$$H = n \int_{0 < R < 1} I(H_R) dR = 5n^3/6 \tag{12}$$

The ratios of intensities of the different classes of RIs are:

$$H/O = 5/4 = 1.25 \tag{13}$$

$$Y/O = 9(N-n)/2n \tag{14}$$

$$Y/H = 18(N-n)/5n \tag{15}$$

The replicon size, *N*, can thus be calculated from *n*, the known size of the fragment analysed, and from either the signal ratio of Ys to bubbles or the signal ratio of Ys to double Ys:

$$N = n (1 + (2/9) (Y/O)) \tag{16}$$

$$N = n (1 + (5/18) (Y/H)) \tag{17}$$

Experimental determination of the total amount of each class of RIs is complicated by their partial overlap on 2D gels. Bubbles are not well resolved from Ys when *R* < 0.3, and double Ys are not well resolved from Ys when *R* < 0.5. We have thus calculated how these measurable portions of the O-arc and the H-arc relate to the total amount of each class of RI by substituting (*R*₁ = 0.3; *R*₂ = 1.0) into equation (8) and (*R*₁ = 0.5; *R*₂ = 1.0) into equation (9), and comparing the respective results with equation (11) or (12). We obtained:

$$S_{(0.3-1.0)}(O) = (1181/2000) O = 0.59 \times O \tag{18}$$

$$S_{(0.5-1.0)}(H) = (4/5) H = 0.8 \times H \tag{19}$$

These two equations allow one to calculate the total amount of each class of RIs even if only a portion of the 2D gel arc can be measured.

All the above equations are also valid for chromosomal replicons, as long as (i) the *n* bp fragment analysed is smaller than the *N* bp replicon to which it belongs, (ii) initiation occurs at random sequences and (iii) fork speed is constant.

The experimental error in measurements of the percentages of different replicative forms cannot be rigorously determined from the limited number of blots obtained for the early stage investigated here. However, we have tentatively estimated it from duplicated or triplicated sets of data generated from later embryos for some fragments (data not shown). In the case of fragments of constant size, we found satisfyingly low (2–10%) variations in these percentages, which translate into a <20% error margin in replicon size estimates. This is consistent with the experiments presented for plasmid DNA (Figure 5 and Table II), which indicate a 10–22% deviation between calculated and actual replicon size. In the case of very polymorphic fragments and/or abundant partial digests, the error margin can be 5–20% higher.

Acknowledgements

We thank G.Pierron, F.Caron, R.Buckle and F.Tchang for critical reading of the manuscript, and R.Reeder for the gift of plasmids. This work was supported by grants from the Association pour la Recherche sur le Cancer, the Ligue Nationale contre le Cancer, the FEGEFLUC and EEC grant no. ERBSC1*CT000677.

References

Adachi, Y. and Laemmli, U.K. (1992) *J. Cell Biol.*, **119**, 1–15.
 Bakken, A., Morgan, G., Sollner-Webb, B., Roan, J., Busby, S. and Reeder, R.H. (1982) *Proc. Natl Acad. Sci. USA*, **79**, 55–60.
 Baldari, C.T., Amaldi, F. and Buongiorno-Nardelli, M. (1978) *Cell*, **15**, 1095–1107.
 Bell, S.P. and Stillman, B. (1992) *Nature*, **357**, 128–134.
 Bénard, M. and Pierron, G. (1992) *Nucleic Acids Res.*, **20**, 3309–3315.
 Benbow, R.M., Zhao, J. and Larson, D.D. (1992) *Bioessays*, **14**, 661–670.
 Berezney, R. and Coffey, D.S. (1975) *Science*, **189**, 291–293.
 Blumenthal, A.B., Kriegstein, H.J. and Hogness, D.S. (1973) *Cold Spring Harbor Symp. Quant. Biol.*, **38**, 205–223.
 Botchan, P.M. and Dayton, A.I. (1982) *Nature*, **299**, 453–456.
 Botchan, P., Reeder, R.H. and Dawid, I.B. (1977) *Cell*, **11**, 599–607.
 Bozzoni, I., Baldari, C.T., Amaldi, F. and Buongiorno-Nardelli, M. (1981) *Eur. J. Biochem.*, **118**, 585–590.
 Brewer, B.J. and Fangman, W.L. (1987) *Cell*, **51**, 463–471.
 Brewer, B.J. and Fangman, W.L. (1988) *Cell*, **55**, 637–643.
 Brewer, B.J., Lockshon, D. and Fangman, W.L. (1992) *Cell*, **71**, 267–276.
 Buongiorno-Nardelli, M., Micheli, G., Carri, M.T. and Marilley, M. (1982) *Nature*, **298**, 100–102.

- Burhans, W.C., Vassilev, L.T., Caddle, M.S., Heintz, N.H. and DePamphilis, M.L. (1990) *Cell*, **62**, 955–965.
- Busby, S.J. and Reeder, R.H. (1982) *Dev. Biol.*, **91**, 458–467.
- Caddle, M.S. and Calos, M.P. (1992) *Nucleic Acids Res.*, **20**, 5971–5978.
- Callan, H.G. (1972) *Proc. R. Soc. London Ser. B*, **181**, 19–41.
- Cook, P.R. (1991) *Cell*, **66**, 627–635.
- Cox, L.S. and Laskey, R.A. (1991) *Cell*, **66**, 271–275.
- Delidakis, C. and Kafatos, F.C. (1989) *EMBO J.*, **8**, 891–901.
- DePamphilis, M.L. (1993) *J. Biol. Chem.*, **268**, 1–4.
- Diffley, J.F.X. and Cocker, J.H. (1992) *Nature*, **357**, 169–172.
- Dijkwel, P.A. and Hamlin, J.L. (1992) *Mol. Cell Biol.*, **12**, 3715–3722.
- Dijkwel, P.A., Vaughn, J.P. and Hamlin, J.L. (1991) *Mol. Cell Biol.*, **11**, 3850–3859.
- Fangman, W.L. and Brewer, B.J. (1991) *Annu. Rev. Cell Biol.*, **7**, 375–402.
- Fangman, W.L. and Brewer, B.J. (1992) *Cell*, **71**, 363–366.
- Gaudette, M.F. and Benbow, R.M. (1986) *Proc. Natl Acad. Sci. USA*, **83**, 5953–5957.
- Goldman, M.A. (1988) *BioEssays*, **9**, 30–35.
- Graham, C.F. and Morgan, R.W. (1966) *Dev. Biol.*, **14**, 439–460.
- Gurdon, J.B. and Wickens, M.P. (1983) *Methods Enzymol.*, **101**, 370–386.
- Hamlin, J.L. (1992) *BioEssays*, **14**, 651–659.
- Harland, R.M. and Laskey, R.A. (1980) *Cell*, **21**, 761–771.
- Heck, M.M.S. and Spradling, A.C. (1990) *J. Cell Biol.*, **110**, 903–914.
- Heintz, N.H. (1992) *Curr. Opin. Cell Biol.*, **4**, 459–467.
- Heintz, N.H., Dailey, L., Held, P. and Heintz, N. (1992) *Trends Genet.*, **8**, 376–381.
- Heinzel, S.S., Krysan, P.J., Tran, C.T. and Calos, M.P. (1991) *Mol. Cell Biol.*, **11**, 2263–2273.
- Hernandez, P., Martin-Parras, L., Martinez-Robles, M.L. and Schwartzman, J.B. (1993) *EMBO J.*, **12**, 1475–1485.
- Huberman, J.A. and Riggs, A.D. (1968) *J. Mol. Biol.*, **32**, 327–341.
- Huberman, J.A., Spotila, L.D., Nawotka, K.A., El-Assouli, S.M. and Davis, L.R. (1987) *Cell*, **51**, 473–481.
- Hutchinson, C.J. and Kill, I. (1989) *J. Cell Sci.*, **93**, 605–613.
- Hyrien, O. and Méchali, M. (1992) *Nucleic Acids Res.*, **20**, 1463–1469.
- Jackson, D.A. (1991) *BioEssays*, **13**, 1–10.
- Kill, I.R., Bridger, J.M., Campbell, K.H.S., Maldonado-Codina, G. and Hutchinson, C.J. (1991) *J. Cell Sci.*, **100**, 869–876.
- Kobayashi, T., Hidaka, M., Nishizawa, M. and Horiuchi, T. (1992) *Mol. Gen. Genet.*, **233**, 355–362.
- Krysan, P.J. and Calos, M.P. (1991) *Mol. Cell Biol.*, **11**, 1464–1472.
- Laskey, R.A. (1985) *J. Embryol. Exp. Morphol.*, **89** (Suppl.), 285–296.
- Leibovici, M., Monod, G., Géraudie, J., Bravo, R. and Méchali, M. (1992) *J. Cell Sci.*, **102**, 63–69.
- Linskens, M.H.K. and Huberman, J.A. (1988) *Mol. Cell Biol.*, **8**, 4927–4935.
- Linskens, M.H.K. and Huberman, J.A. (1990) *Cell*, **62**, 845–847.
- Mahubani, H.M., Paull, T., Elder, J.K. and Blow, J.J. (1992) *Nucleic Acids Res.*, **20**, 1457–1462.
- Martin-Parras, L., Hernandez, P., Martinez-Robles, M.-L. and Schwartzman, J.B. (1992) *J. Biol. Chem.*, **267**, 22496–22505.
- McKnight, S.L., Bustin, M. and Miller, O.L. (1978) *Cold Spring Harbor Symp. Quant. Biol.*, **42**, 741–754.
- Méchali, M. and Kearsley, S. (1984) *Cell*, **38**, 55–64.
- Micheli, G., Baldari, C.T., Carri, M.T., Di Cello, G. and Buongiorno-Nardelli, M. (1982) *Exp. Cell Res.*, **137**, 127–140.
- Mills, A.D., Blow, J.J., White, J.G., Amos, W.B., Wilcock, D. and Laskey, R.A. (1989) *J. Cell Sci.*, **94**, 471–477.
- Mirkovitch, J., Mirault, M.-E. and Laemmli, U.K. (1984) *Cell*, **39**, 223–232.
- Montag, M., Spring, H. and Trendelenburg, M.F. (1988) *Chromosoma*, **96**, 187–196.
- Müller, B., Burdett, I. and West, S.C. (1992) *EMBO J.*, **11**, 2685–2693.
- Nakamura, H., Morita, T. and Sato, C. (1986) *Exp. Cell Res.*, **165**, 291–297.
- Nakayasu, H. and Berezney, R. (1989) *J. Cell Biol.*, **108**, 1–11.
- Newport, J. and Kirschner, M. (1982) *Cell*, **30**, 675–686.
- Pardoll, D.M., Vogelstein, B. and Coffey, D.S. (1980) *Cell*, **19**, 527–536.
- Reeder, R.H. (1990) *Trends Genet.*, **6**, 390–395.
- Sambrook, J., Fritsch, E.F. and Maniatis, T. (1989) *Molecular Cloning: A Laboratory Manual*. Cold Spring Harbor Laboratory Press, Cold Spring Harbor, NY.
- Satoh, N. (1977) *Dev. Growth Diff.*, **19**, 111–117.
- Shinomiya, T. and Ina, S. (1991) *Nucleic Acids Res.*, **19**, 3935–3941.
- Shiokawa, K., Misumi, Y. and Yamana, K. (1981) *Dev. Growth Diff.*, **23**, 579–587.
- Signoret, J. and Lefresne, J. (1971) *Ann. Embryol. Morphogen.*, **4**, 113–123.
- Stinchcomb, D.T., Struhl, K. and Davis, R.W. (1979) *Nature*, **282**, 39–43.
- Tran, C.T., Caddle, M.S. and Calos, M.P. (1993) *Chromosoma*, **102**, 129–136.
- van der Velden, H.M.W. and Wanka, F. (1987) *Mol. Biol. Rep.*, **12**, 69–77.
- Van't Hof, J. and Lamm, S.S. (1991) *EMBO J.*, **10**, 1949–1953.
- Vassilev, L.T., Burhans, W.C. and DePamphilis, M.L. (1990) *Mol. Cell Biol.*, **10**, 4685–4689.
- Vaughn, J.P., Dijkwel, P.A. and Hamlin, J.L. (1990a) *Cell*, **61**, 1075–1087.
- Vaughn, J.P., Dijkwel, P.A., Mullenders, L.H.F. and Hamlin, J.L. (1990b) *Nucleic Acids Res.*, **18**, 1965–1969.
- Wolffe, A.P. (1992) *Chromatin: Structure and Function*. Academic Press, London.
- Zhu, J., Newlon, C.S. and Huberman, J.A. (1992a) *Mol. Cell Biol.*, **12**, 4733–4741.
- Zhu, J., Brun, C., Kurooka, H., Tanagida, M. and Huberman, J.A. (1992b) *Chromosoma*, **102** (Suppl.), 7–16.

Received on June 30, 1993; revised on August 17, 1993

Note added in proof

The replication of the human rDNA cluster has recently been analysed in cultured cells by 2D electrophoresis [Little, R.D., Platt, T.H.K. and Schildkraut, C.L. (1993) *Mol. Cell Biol.*, **13**, in press]. Initiation occurs at multiple sites throughout the intergenic spacer but not within the transcription unit. The comparison with *Xenopus* blastulae suggests that active transcription may prevent initiation of DNA replication within the transcription unit sequences.